Mine-used Flameproof Inverter Heat Dissipation Design and Its Performance Analysis

Yue Wang [1, 2, *], Xiang Rong [1, 2]

[1] Tiandi (Changzhou) Automation Co., Ltd, Changzhou, China.
[2] CCTEG Changzhou Research Institute, Changzhou, China.

Abstract—Flameproof inverter for mine-used have a significant warming effect during operation, resulting in reduced reliability and susceptibility to thermal degradation and thermal failure. However, there is a lack of thermal analysis research on the operation mechanism and process evaluation of mining inverters. This paper analyzes the electrical characteristics of internal power devices and calculates the power loss. Secondly, on the basis of comparing the influence of flow rate, structural parameters and installation location on the thermal performance, the forced water cooling + air cooling + natural cooling method is used to optimize the design of the thermal system. Finally, ANSYS Icepak is used to conduct a comprehensive numerical simulation analysis of the internal temperature field characteristics and convective heat transfer characteristics. The simulation verifies the effectiveness of the heat dissipation-based design, and the results show that: the internal components of the mining explosion-proof inverter are not more than 80 ℃, which is much lower than the value specified in the relevant standards, and it has a good heat dissipation performance, which effectively guarantees the safe, stable and reliable operation of the mining explosion-proof inverter.

1. Introduction

Mine-used flameproof inverter plays a vital role in promoting intelligent mining in coal mines, enhancing safe coal mine production, and helping coal mines to develop in a green way [1]. Its compact internal structure, variable working conditions and high power density lead to significant heating effects, reduced reliability and susceptibility to thermal degradation and thermal failure [2-3]. Therefore, the thermal performance of mine-used flameproof inverter is particularly important.

[4]analyzed the temperature and fluid distribution of contactor and busbar under normal working conditions and fan failure conditions. In [5], the temperature field distribution of transformer winding is obtained by finite element thermal-flow coupling calculation. [6] simulated the temperature rise process of the reactor and the temperature field distribution at steady state. In addition, the researchers also used finite element software to design and optimize the key parameters of fin radiator [7], heat pipe radiator [8] and water-cooled radiator [9]. However, the above research is a separate analysis of a certain type of power device or radiator, and there are many power devices in the mine-used flameproof inverter, and the heat exchange between them should be considered, and there are a variety of heat dissipation methods mixed application.

In this paper, the electrical characteristics of internal power devices are analyzed, and the power loss is calculated according to the relevant theory. On the basis of comparing the influence of flow rate, structural parameters and installation position on heat dissipation performance, the heat dissipation system is optimized by forced water cooling + air cooling + natural cooling. Finally, ANSYS Icepak is used to conduct a comprehensive numerical simulation analysis of the internal temperature field characteristics and convective heat transfer characteristics, and the effectiveness of the heat dissipation design is verified.

2. Loss Analysis of Internal Power Devices

In this paper, a 630kW/1140V four-quadrant mine-used flameproof inverter is taken as the research object. Among them, vacuum AC contactor, busbar, IGBT module and output filter are not only large power consumption devices, but also high thermal sensitivity devices, which need to be considered in the design process of heat dissipation system.

2.1. The power loss of IGBT module

The power loss of IGBT module mainly includes IGBT on-state loss, turn-on and turn-off loss and freewheeling diode loss. According to the electrical performance

* Corresponding author: m18635372893@163.com

parameters and output characteristic curve, the theoretical calculation is carried out[10]. The method is as follows:

The on-state loss of IGBT module is :

$$P_{\text{cond,IGBT}} = \frac{1}{T_0}\int_0^{T_0/2}\frac{1}{2}\left(V_{CE0} + r*i(t)\right)*I\sin(\omega t)*\left(1+m\sin(\omega t+\varphi)\right)dt \tag{1}$$

The turn-on and turn-off losses of IGBT module are :

$$P_{\text{SW,IGBT}} = \frac{1}{\pi}*f_{\text{SW}}*\left(E_{\text{on,IGBT}}(I_{\text{nom}},V_{\text{nom}}) + E_{\text{off,IGBT}}(I_{\text{nom}},V_{\text{nom}})\right)*\frac{I}{I_{\text{nom}}}*\frac{U_{\text{dc}}}{U_{\text{nom}}} \tag{2}$$

In the formula, U_{CEO} is the threshold voltage, r is the slope resistance; $\tau'(t)$ is the duty cycle of the inverter bridge output; m is the modulation ratio; φ is the phase difference between the output signal and the current; f_{sw} is the switching frequency of IGBT module; Eon, IGBT, Eoff, IGBT are the turn-on and turn-off losses of IGBT under rated conditions, respectively; U_{nom} and I_{nom} are the reference voltage and reference current of IGBT module respectively; I is the output current value of the inverter unit; U_{dc} is the DC bus voltage.

The power loss of the diode is:

$$P_{\text{DIODE}} = \frac{1}{\pi}*f_{\text{SW}}*\left(E_{\text{rec}}(I_{\text{nom}})*(0.45*\frac{I}{I_{\text{nom}}}+0.55)\right)*\frac{U_{\text{dc}}}{U_{\text{nom}}} \tag{3}$$

In the formula, E_{rec} is the turn-off loss of the diode under rated conditions.

According to the formula (1) - (3), combined with the data manual, the power loss of FZ800R33KF2C IGBT module at 125 ℃ junction temperature is 1700 W.

2.2. Power loss of busbar

According to formula (4), considering the skin effect of the connecting busbar, the power loss is calculated by combining the measured resistance value of the bridge tester.

$$P_{\text{m}} = K_{\text{jf}}I^2R = \left(\frac{S}{186}\right)^{0.1}I^2R \tag{4}$$

In the formula: K_{jf} is the skin effect coefficient; I is the rated current of the inverter; R is the resistance value of the busbar; S is the cross-sectional area of the busbar.

According to the calculation, the power loss of the positive phase, negative phase and U / V / W phase of the AC busbar is 5.8 W, 0.7 W and 5.2 W respectively. Similarly, the power loss of the positive and negative phases of the AC-DC connection bus is 19.5 W and 14.7 W; the power loss of the positive and negative phases of the DC connection busbar is 5 W and 5 W; the power loss of the unidirectional output copper bar is 2.5 W.

2.3. Power loss of output filter

The output filter device is composed of reactor and RC absorption circuit. For the absorption resistor, the total power loss is calculated to be 300 W [11].

For the reactor, it can be obtained from the selection manual that the load loss of the reactor is 260 W and the no-load loss is 30 W. At the same time, considering the influence of load fluctuation, the winding loss and core loss of the reactor are 270 W and 30 W respectively, and the power loss is 300 W.

$$P = P_{\text{Cu}} + P_{\text{Fe}} = K_{\text{T}}P_{\text{k}} + P_0 \tag{5}$$

In the formula: $\triangle P$ is the active power loss of the transformer; P_{Cu} is winding loss; P_{Fe} is the core loss; K_{T} is the load fluctuation loss coefficient, take 1.05; P_{k} is load loss; P_0 is no-load loss.

2.4. Power loss of vacuum AC contactor

The vacuum AC contactor includes three models : 80A / 1140V, 160A / 1140V and 630A / 1140V. The pull-in time is very short, only 30 ms. Therefore, the thermal effect of the pull-in process is not analyzed in this paper. After suction, the power loss is measured by the holding power. According to the selection manual, the holding power of the aforementioned vacuum AC contactor is 10 W, 18 W, and 15 W, respectively.

3. Design of Heat Dissipation System

The IGBT module and the absorption resistors are cooled by water, the reactor is cooled by air, and the other power devices are cooled by natural cooling.

3.1. Design of Water-cooled Radiator

The thermal performance of different materials, different flow rates, and different channel-substrate distances were comparatively analyzed, and the relationship surface between the above conditions and the maximum temperature of the IGBT module and absorbing resistor was obtained, as shown in Fig. 1.

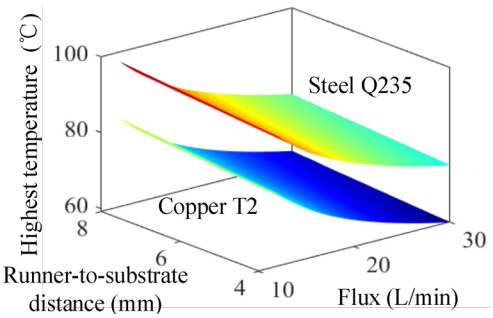

Fig.1 The highest temperature of IGBT module and absorption resistor under different conditions

From fig. 1, it can be seen that under the same conditions, the heat dissipation performance of copper is better than that of steel, but the bearing capacity of steel is better than that of copper, and the material and processing cost of copper is high. In order to meet the same heat dissipation performance, it is necessary to increase the cooling water flow and reduce the distance from the flow channel to the surface. The design requires the IGBT

module and the absorption resistor to have a maximum junction temperature of 75 ℃.Therefore, the cooling water flow rate is selected to be 30 L/min, and the distance from the channel to the substrate is 4 mm. At this time, the temperature field distribution of water-cooled radiator, IGBT module and absorption resistors are shown in fig.2.

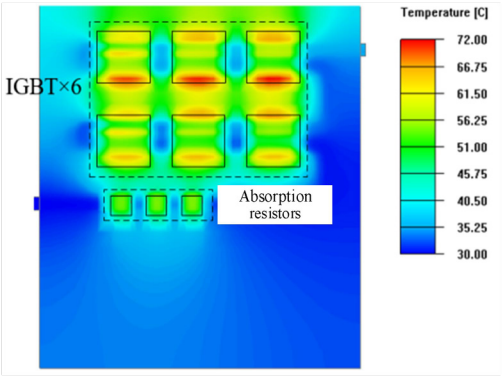

Fig.2 Cloud diagram of temperature distribution of water-cooled radiator, IGBT module and absorption resistor

3.2. Fan Selection and Arrangement

It is assumed that the temperature in the flameproof shell is 40 ℃ when the reactor is in operation. The design requires that the temperature rise does not exceed 30 K. According to the principle of heat transfer, the flow rate of the fan that meets the heat dissipation requirements is:

$$L = Q/\left(C_{\mathrm{P}} \cdot \rho \cdot \Delta T\right) \tag{6}$$

In the formula, Q is the heat transferred from the heat sink to the environment in unit time; C_{P} is the specific heat capacity of air; ρ is air density.

It can be seen from the Section 1 that the total power loss of the reactor is 300 W. Therefore, when Q=300 W, air density ρ=1.128 kg/m at 40 °C, and air specific heat capacity C_{P}=0.2814 Wh/(kg K) at 40 °C are substituted into formula 6, the fan flow rate is 30 m^3/h.

Comparing the influence of transverse and longitudinal air inlet on the heat dissipation performance of the reactor, the temperature field distribution of the reactor in different air inlet directions is obtained, as shown in Fig.3.

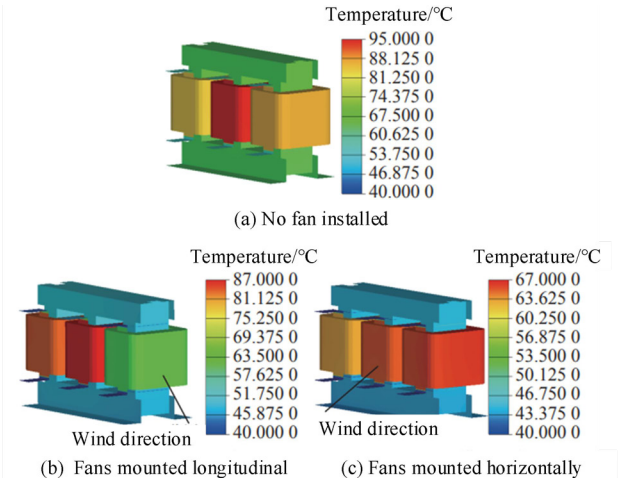

Fig.3 Reactor temperature distribution in different air inlet directions

It can be seen from Fig.3 that the temperature rise of longitudinal air inlet is 7 ℃ higher than that of transverse air inlet, and the heat dissipation effect of transverse air inlet is better.

4. Temperature Field Simulation Analysis

The integrated model for research is shown in Fig.4. Except that the reactor and the absorption resistors are arranged on the left side, and the vacuum AC contactor is arranged on the right side, the remaining power devices are symmetrically arranged.

ANSYS Icepak is used to conduct a comprehensive numerical simulation analysis of the internal temperature field characteristics and convective heat transfer characteristics. The power loss is substituted into the finite element model and the corresponding material properties are configured. When the ambient temperature is 30 ℃, the temperature field distribution of the flameproof shell and internal components is shown in Fig.5 and 6.

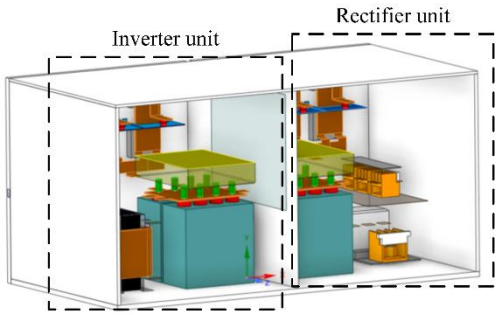

Fig.4 Integrated model of mine-used flameproof inverter

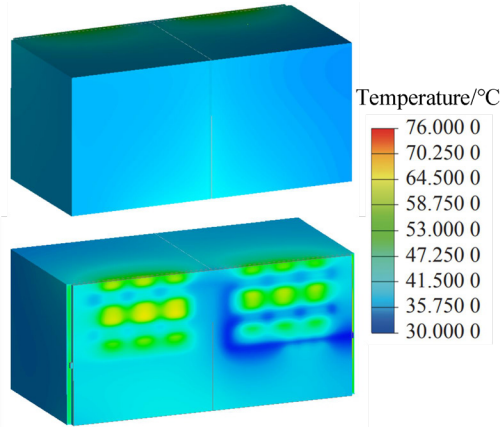

Fig.5 Cloud map of temperature field distribution of flameproof shell

It can be seen from Fig.5 that due to the conduction, convection and radiation heat transfer of the internal power device, the temperature of the flameproof shell is higher than the ambient temperature, the lowest is 36 ℃,

and the temperature of the rear substrate is higher than other flameproof surfaces, up to 70 °C.

It can be seen from Fig.6 that the temperature of the IGBT module is the highest, followed by the core busbar assembly, and the temperature of the DC filter capacitor assembly is the lowest. For Fig.6 (a), because the two water-cooled radiators are connected in series, the temperature increases with the extension of the cooling water flow path, resulting in the temperature of the IGBT module on the inverter side higher than that on the rectifier side. For Fig.6 (b) and (d), the temperature of the AC-DC busbar is higher than that of the AC busbar, the temperature of the output copper busbar is the lowest, and the temperature of the core busbar assembly on the inverter side is higher than that on the rectifier side. The temperature difference between the two is mainly reflected in the AC-DC busbar. Because the absorption resistors are located on the inverter side, the temperature of the AC-DC busbar adjacent to it will increase under the action of radiation heat transfer. For Fig.6 (c) and (e), the temperature of the DC filter capacitor component on the rectifier side is higher than that on the inverter side. It can be seen that the longitudinal air inlet can also play a role in heat dissipation. For Fig.6 (f), the 80A / 1140V AC contactor has a larger power density and denser arrangement, and the temperature rise is higher than that of the 630A / 1140V AC contactor. Although the 160A / 1140V vacuum AC contactor does not work, there is still a temperature rise phenomenon under the action of conduction and radiation heat transfer. For Fig.6 (g), the temperature of the reactor is higher than the individual analysis value given in Fig.3. This is due to the heat exchange between the internal power devices.

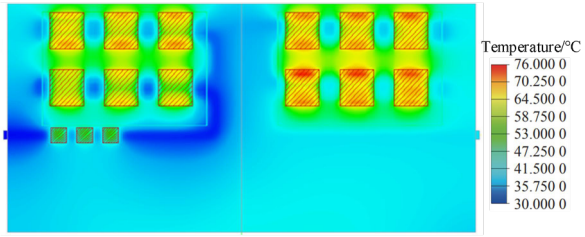

（a）Water-cooled heat sinks, IGBT modules and absorber resistors

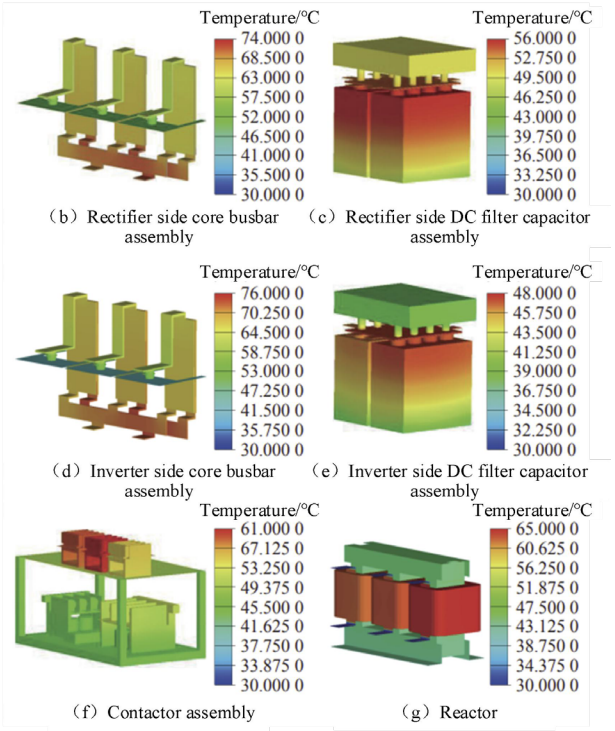

（b）Rectifier side core busbar assembly （c）Rectifier side DC filter capacitor assembly

（d）Inverter side core busbar assembly （e）Inverter side DC filter capacitor assembly

（f）Contactor assembly （g）Reactor

Fig.6 Temperature field distribution cloud diagram of internal components of flameproof shell

On the whole, the internal components of the mine flameproof frequency converter do not exceed 80 °C, which is far lower than the specified value of the relevant standards. It has good heat dissipation performance and can provide guarantee for the safe, stable and reliable operation of the mine-used flameproof inverter

5. Conclusions

A. The electrical characteristics of internal power devices are analyzed and the power loss is calculated. The power loss of IGBT module, absorption resistor and reactor is higher than that of other power devices.

B. The mixed heat dissipation method of water cooling + air cooling + natural cooling is adopted: the selected material is Q235 steel, the cooling water flow is 30L / min, and the distance from the flow channel to the substrate is 4mm ; the temperature rise of longitudinal air inlet is 7 °C higher than that of transverse air inlet.

C. The simulation verifies the effectiveness of the heat dissipation design: the temperature of the internal components does not exceed 80 °C. Among them, the temperature of the IGBT module is the highest, the temperature of the core busbar component is the second, and the temperature of the DC filter capacitor component is the lowest.

Acknowledgment

This research is co-supported by the Special Fund for the Technology Innovation and Entrepreneurship of Tiandi Company Ltd. (Grant nos. 2023-TD-MS005 and 2023-TD-ZD001-006). And the Tiandi (Changzhou) Automation Co., Ltd. R&D project (2023GY1002). The authors would like to thank them.

References

1. ZHU Yongping,XU Xiaojian.Development trend of mine frequency converter[J].Industry and Mine Automation, 2017,43(10):18-23.
2. Ryu, T.; Choi, U.-M.; Vernica, I.; Blaabjerg, F. Effect of thermal loading definitions on the mission profile-based reliability evaluation of power devices in PV inverters. Microelectronics Reliability 2022, 138, 114650.
3. YANG Weilin.Brief discussion on heat dissipation design of explosion-proof frequency inverter[J].Explosion-Proof Electric Machine,2019,54(1):36-39,42.
4. LIU Sijun,HAN Wei,ZHANG Haixing,et al.Research on temperature fluid field simulation and heat dissipation optimization of high voltage switchgear[J].High Voltage Apparatus,2020,56(10):63-69.
5. GU Shengjian,YOU Piaopiao,JIANG Youhua.Thermal performance analysis of dry-type transformer under condition of non-ideal power supply[J].Transformer, 2020, 57(6):19-24.
6. LI Jinzhong,ZHANG Dandan,XU Zhengyu,et al.Heat dissipation performance of ultra-high voltage shunt reactor with sound insulation based on finite element method[J]. High Voltage Engineering,2017,43(3):822-827.
7. XUPengcheng,TAO Hanzhong,ZHANG Hong. Optimization and analysis of IGBT heat pipe heat sink with integral fin[J].Journal of Refrigeration,2014,35(5):101-104,109.
8. DING Jie,ZHANG Ping.Temperature rise test and thermal simulation of heat-pipe radiator of metro vehicel traction inverter[J].China Railway Science,2016,37(3):95-102.
9. YIN Yuxing,ZHU Zhaoxia.Research of water cooling performance of mine flameproof frequency converter[J]. Coal Mine Machinery,2015,36(8):83-85.
10. Das, S. C.; Narayanan, G.; Tiwari, A. Experimental study on the influence of junction temperature on the relationship between IGBT switching energy loss and device current. Microelectronics Reliability 2018, 80, 134–143.
11. RONG Xiang，SHI Han，JIANG Dezhi, et al. A mine-used frequency converter filter device[J].Industry and Mine Automation,2020,46(5):76-81.